FAILURE OF SEABEDS WITH A HIGH MUD CONTENT: AN EXPERIMENTAL STUDY

Valeria Chávez[1], Edgar Mendoza[1], Rodolfo Silva[1], Ana Meneses[2], Dulce Perez[3], María Clavero[4], Izaskun Benedicto[3] and Miguel Losada[4]

Seabed instability has been cited as the cause of failure for a number of coastal structures in recent years, stimulating an interest in understanding the interaction between waves, marine structures and the seabed upon which they are built. A series of experimental tests were carried out in a wave flume at the Engineering Institute of the National University of Mexico, to investigate the failure of seabeds with a high mud content and the interaction of the seabed with a scaled structure (vertical breakwater) and regular waves (T = 0.6, 0.8 and 1.0 s; H = 6, 8 and 10 cm), through the analysis of pore pressure distribution. Three different materials were tested: 100, 90 and 85 % mud content, mixed with natural sand and water. Pore pressure build-up was registered in the tests with 85 % of mud content, and knowing that a build-up precedes soil liquefaction, failure may have occurred. But in these cases the maximum pressure in the tests did not exceed the critical value and no liquefaction was observed. For soils of 90 and 100 % mud content, the pore pressure shows a homogeneous vertical behaviour and only pore pressure falls were registered. This phenomenon may be attributed to the cohesion effect in the mud particles and to the consolidation process.

Keywords: wave-induced pore pressure, liquefaction, vertical breakwater

INTRODUCTION

Soil liquefaction has been observed in various natural seabed conditions. It takes place when pore pressure within the seabed (undrained soils) is exceeded due to dynamic and/or static overloads. The increase of the pore pressure can be heightened by the presence of a marine structure which acts in two ways, firstly inducing pressure to the whole system and secondly blocking the water to be released, thus worsening the undrained condition. The instability of the seabed in the area below and surrounding the structure may result in its total collapse, as has been demonstrated by several accidents on breakwaters, pipelines and oil platforms. The process of induced soil instability can be considered a geotechnical failure mode for a marine structure. One example of this occurred in Barcelona Harbour, in 2001, when the top of four caissons of a dyke, which was under construction, tilted in the seaward direction during a storm (Figure 1). Prior to the placement of the caissons part of the soft silts and silty clays of the seabed were taken out and frictional material was set instead to improve the caisson stability. According to Puzrin *et al*. (2010), the sinking of the caissons can be explained by a strength-loss mechanism in the soil, due to the dynamic loading exerted by the waves combined with the weight of the caissons. The analysis of the soil liquefaction, indicates that extensive zones of the caisson foundation reached critical stress values during the storm.

Figure 1. Barcelona Harbour, Spain: 2001 (Puzrin *et al*., 2010)

A second example occurred in 2007, in Mexico, when a cold front affected the Sonda of Campeche, in the Gulf of Mexico. The Usumacinta drilling platform (MAT-Cantiliver type) was subjected to large waves generated by winds of over 100 km/h, resulting in the oscillation and settling of the platform, and the collision of the cantilever deck (Figure 2). The subsequent investigation into the disaster, carried out by Batelle, stated that the main cause of the accident was the seabed instability (mostly composed of clay), induced by the extreme wave action (Petróleos Mexicanos, 2008).

[1] Engineering Institute, UNAM, Ciudad Universitaria, Mexico City, 04510, Mexico
[2] Aleph Ingenieros Consultores, Amores 50, Mexico City, 03100, Mexico
[3] PROES Consultores, General Yagüe 39, Madrid, 28020, Spain
[4] University of Granada, Real de Cartuja 36, Granda, 18012, Spain

Figure 2. Usumacinta platform, Mexico: 2007 (PEMEX, 2008)

Another documented case was the failure of a platform in the Shengli offshore oil field (Figure 3), on the delta of the Yellow River, China, in 2010. The seabed here is mainly constituted by silty soil with a coarse sand layer at the surface. During the passage of typhoon Malou, in the Bohai Sea, heavy waves induced pore pressure accumulation in the seabed and soil liquefaction (Zhu, 2013). The platform inclined to over 45 degrees, causing four workers to fall into the water and trapping thirty two of them on the platform.

Figure 3. Shengli Oilfield No. 3 drilling platform, China: 2010 (Xinhua Photo, http://english.sina.com)

Clearly, the three accidents described above have common elements which are: a seabed composed mainly of fine sediments (silt or clay), the placement of a structure on the seabed (artificial static load) and the occurrence of energetic waves (dynamic extreme load). In this sense, the wave-induced increase in the pore pressure over time, the lack of drainage and the overload in the seabed seem to be the key factors for liquefaction to occur.

The importance of the liquefaction process has led to the experimental and analytical studies carried out since the 1940's (Jeng, 2013) while investigations of seabed-structure interaction have also been carried out recently (Mostafa *et al*, 1999; Sumer *et al*, 1999; Kudella *et al*., 2006; Sumer *et al*., 2006; Kirca, 2013). But to the best of the authors' knowledge, small scale experiments of a structure exerting a static overload on a seabed with a high mud content exposed to wave action have not been tested, nor a detailed spatial distribution of the pore pressure been reported. The presentation of the latter is the main objective of this paper.

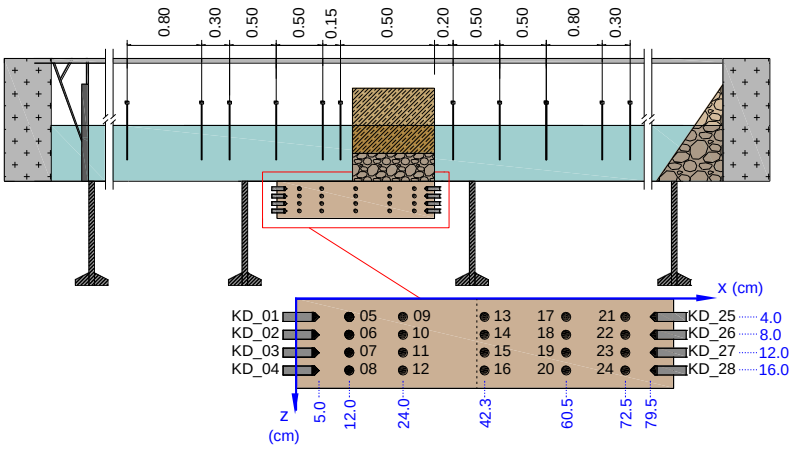

Figure 4. Experimental set-up

EXPERIMENTAL SET-UP

Wave flume and instrumentation

A flume of 22 m length, 0.60 m depth, and 0.40 m width at the Engineering Institute of the National University of Mexico was used for the experiments. The soil was placed 13 m away from the wave paddle, flush with the flume bottom, in an acrylic pit 20 cm deep and 84.5 cm long. Twenty eight pressure transmitters were distributed on three lateral faces of the pit (left, right and back faces) and eleven wave gauges were placed along the length of the flume. The instrumentation and the reference system selected are shown in Figure 4. The measurements were acquired and synchronized using an imc SPARTAN data logger. The facilities and instrumentation were the same as those reported by Chávez, 2014.

Vertical breakwater

A small scale structure of 140 kg, representing a vertical breakwater, was placed over the bed. The dimensions of the model were 44 cm length and 50 cm height. The rubble mound foundation of the vertical breakwater was represented by a 15 cm gravel layer held in place by a rectangular, mesh box. The superstructure was formed by a 35 cm, impermeable wood case filled with concrete cubes (Figure 5). The leeward side of the structure was aligned with the border of the pit, as shown in Figure 4 and Figure 5.

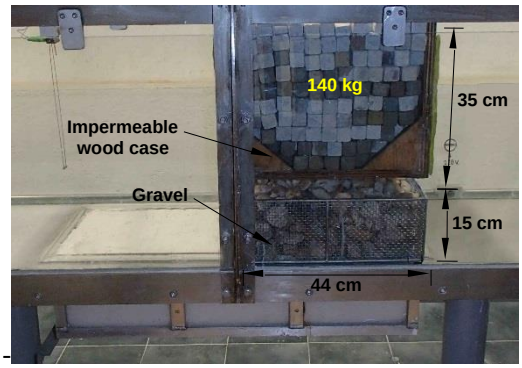

Figure 5. Scaled vertical breakwater

Mud characteristics

The tested mud layers were fabricated “in-house”, mixing commercial kaolinite (fine material) and natural sand (granular material) from Puerto Morelos, Quintana Roo, Mexico in 90-10 % and 85-15 % proportions. The mixtures were prepared with different solid-water concentrations, as shown in Table 1. The particle size distributions for the soils are presented in Figure 6.

Table 1. Tested mud characteristics

Mud-granular material concentration	Material ID	d_{50} (mm)	Solid-water (kg/L)
100 % kaolinite	100C	0.00170	3.1
90 % kaolinite – 10 % sand	90C10A	0.00256	3.1
85 % kaolinite – 15 % sand	85C15A	0.00222	2.5

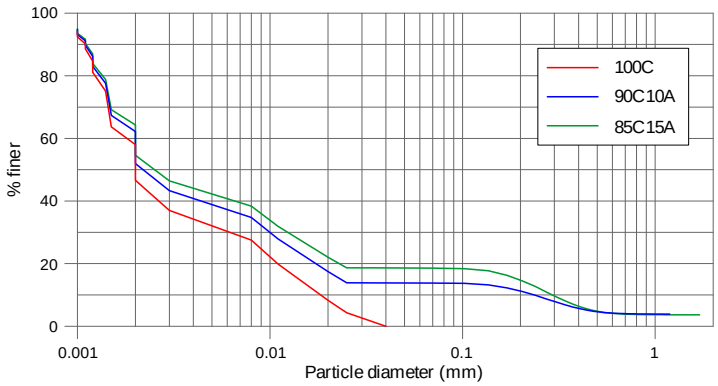

Figure 6. Particle size distribution of the tested soils

EXPERIMENTAL PROCEDURE

The methodology followed for each experiment was:

1. Prepare the mud by rubbing until a homogenous mixture is obtained.
2. Fill the pit flush with the bottom of the flume.
3. Let the soil consolidate until it is able to bear the structure weight.
4. Fill the flume with 30 cm of water and build the structure.
5. Allow the system to consolidate for 24 hours.
6. Calibrate the wave gauges.
7. Set the pressure transmitters to zero.
8. Switch on the measurement system and start the waves (only monochromatic wave trains were generated). Table 2 shows the wave conditions tested, in which a set of two periods with three wave heights each is called a Phase.
9. After 12 hours, repeat steps 6 to 8 to run a new Phase.

Four experiments were carried out with the three different muds; the wave conditions selected and the experiment characteristics are shown in Table 2.

Table 2. Experimental wave conditions

Experiment	Material	T (s)	H (cm)	Time per wave train (min)	Number of Phases
1	100C	0.8	6, 8 and 10	20	3
		0.6	6, 8 and 10	20	
2	90C10A	0.6	6, 8 and 10	40	2
		0.8	6, 8 and 10	40	
3	85C15A	0.8	6, 8 and 10	20	1
		1.0	6 and 8	20	
4	85C15A	0.8	6, 8 and 10	20	4
		1.0	6, 8 and 10*	20	

*In phases 2 to 4 of Experiment 4, for T=1.0 s, the wave height of 10 cm was not run because the reflection induced by the vertical structure produced wave breaking

RESULTS

100 % mud content (100C)

The contour maps presented in Figure 7 show the maximum pore pressure (averaged in a wave period) for the wave heights corresponding to T = 0.8 s of Experiment 1. These contour maps were constructed using the 28 pore pressure time-series registered by the transmitters and considering all the measurement points as part of the same XZ plane (transmitters KD01 to KD04 and KD25 to KD28 were displaced 0.07 m in the Y direction from the others). These maps show a homogeneous vertical distribution of the pressure. In the area beneath the structure (seaward limit at x = 40.5 cm), the weight of the structure makes the pore water drain away and thus the pressure begins to decrease. As the waves can barely propagate through the mud, drainage increases at the leeward side of the structure and the pit. Given that the pit is made of acrylic, the leeward end lets the mud layer drain, this can be observed in the three maps of Figure 7 where a pressure decrease of 5 cm can be seen at the right end of the pit. In contrast, in the area where there is no deadweight (x < 40.5 cm), the pressure distribution does not vary significantly during this phase of the test. This indicates that the consolidation process caused by the weight of the soil itself did not induce a significant variation in the pore pressure.

The time-series shown in Figure 8 confirm that the magnitude of the residual pore pressure shows a constant vertical distribution as the values recorded by pressure transmitters, placed at different mud depths, was identical. At x = 12 cm, where wave action is exerted directly on the mud, a pressure variation resulting from the oscillation of the free surface is observed, but there is no accumulation or loss as it tends to return to the initial value. On the other hand, beneath the structure (x > 40.5 cm), the pressure decreases gradually and independently of wave action. As there is no increase in pore pressure, there is no chance of soil liquefaction in this material. As seen in the time-series, the gradient of pressure loss is the greatest for H = 6 cm, it decreases for H = 8 cm, and the pressure tends to a constant value for H = 10 cm. This phenomenon may be due to the pressure induced by the weight of the structure, which combined with the stresses induced by waves, stabilizes the soil consolidation.

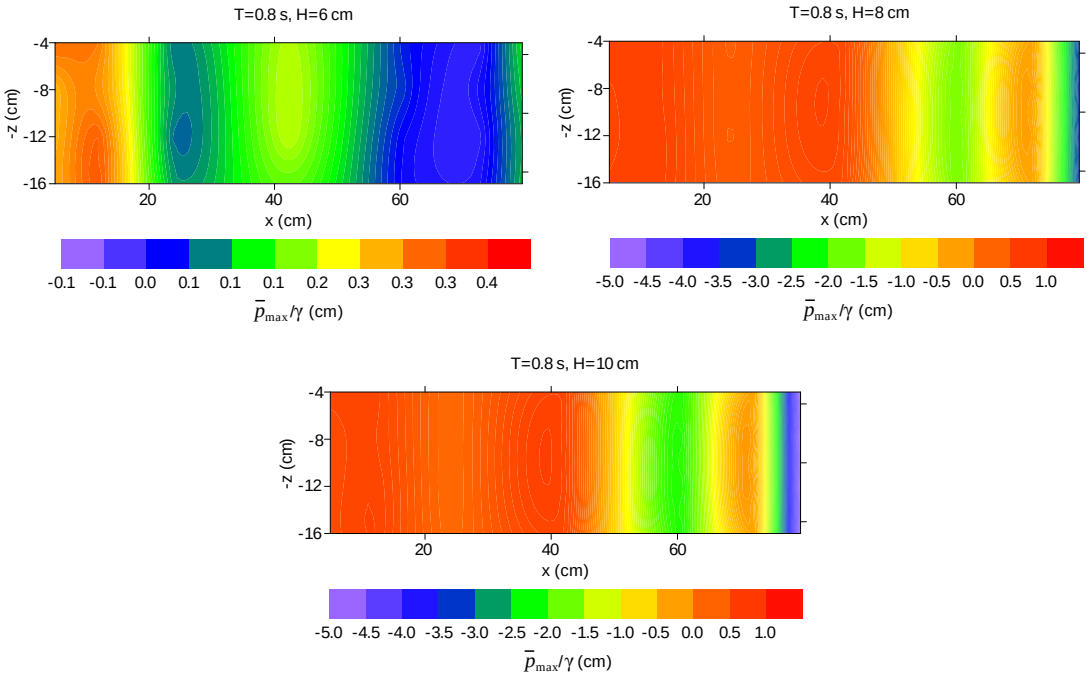

Figure 7. Maximum period averaged pore pressure for Experiment 1 - Phase 1, 100C

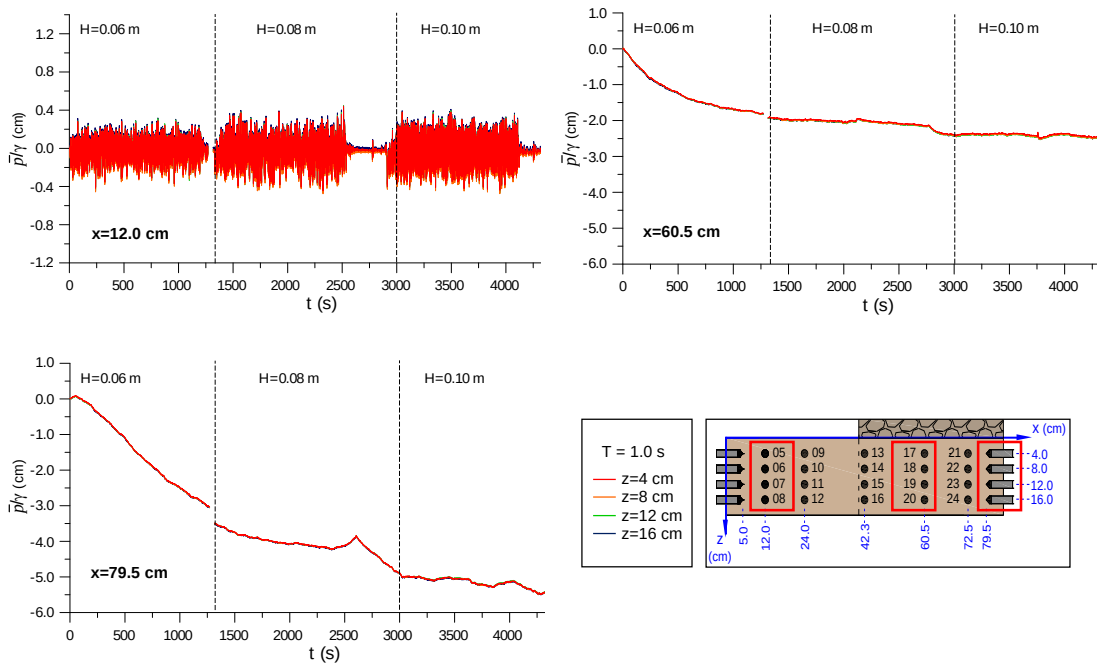

Figure 8. Period averaged pore pressure time-series for Experiment 1 - Phase 1, 100C

90 % mud content (90C10A)

For the first wave period of Phase 1 (T = 0.6 s; H = 0.6, 0.8 and 0.10 s) of Experiment 2, the maximum period averaged pore pressures for each wave height are shown in Figure 9. The figures show a similar pressure distribution to that of 100 % mud content: no relevant variation was seen in the residual mechanism outside the structure (x < 40.5 cm). Beneath the structure (x > 40.5 cm) there was a gradual decrease, with the lowest values found in this section.

In the time-series seen in Figure 10 behaviour similar to that of 100 % mud content is observed. In this case, at x = 79.5 cm (leeward end of the pit), there is gradual decrease in pore pressure, independent

of the wave action (a change is not identified in the gradient with increasing wave height). While this is observed in all the records, for the depth of 16 cm there is a greater gradient of pressure release.

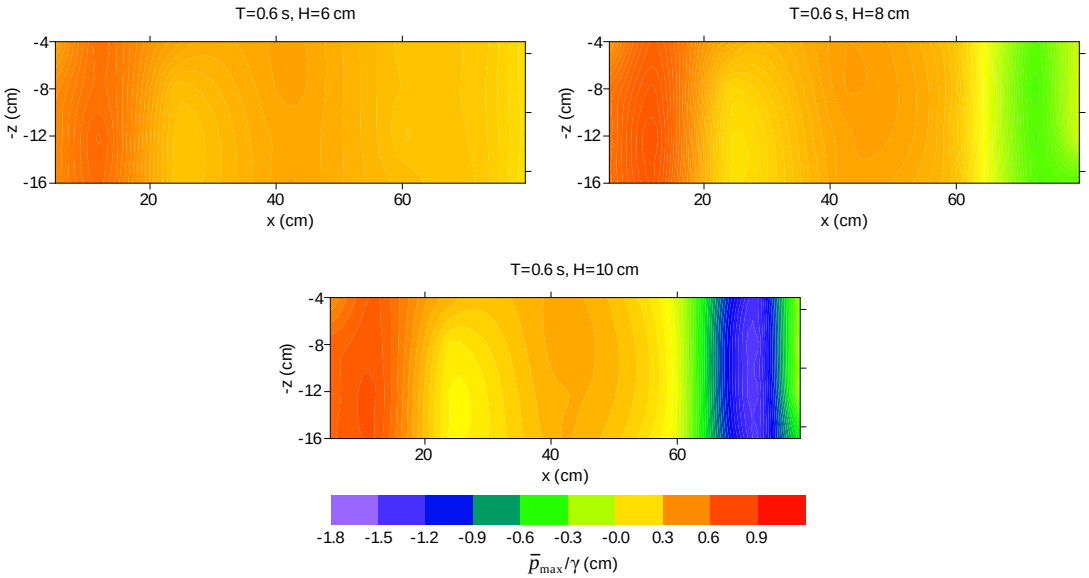

Figure 9. Maximum period averaged pore pressure for Experiment 2 - Phase 1, 90C10A

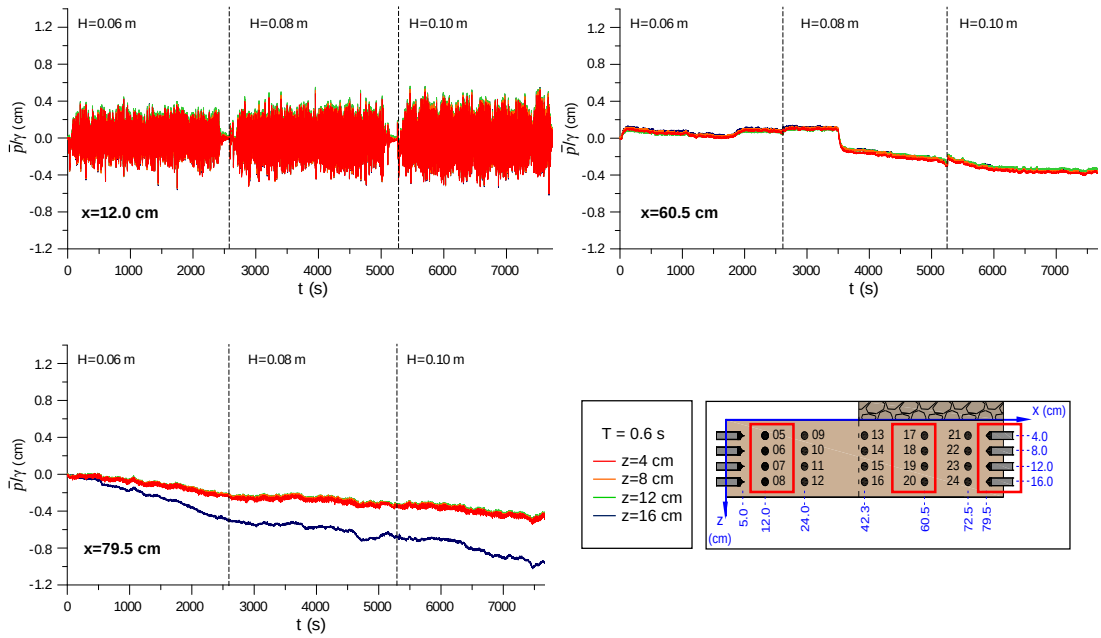

Figure 10. Period averaged pore pressure time-series for Experiment 2 - Phase 1, 90C10A

85 % mud content (85C15A)

Experiment 3 consisted of only one phase, with a wave period 0.8 s, wave heights of 6, 8 and 10 cm, and 1.0 s wave period with wave heights of 6, and 8 cm.

As can be seen in the contour maps of Figure 11 for $T = 0.8$ s the maximum pressure varies vertically, having the highest values at the bottom. As x increases, the pressure decreases and beneath the structure the lowest values were recorded. On the other hand, as H increases, the pressure reaches higher values. For the tests with T=1 s it is observed that by reducing the frequency, the pressure decreases, even presenting negative values for H = 8 cm, thus this mud is not prone to liquefaction.

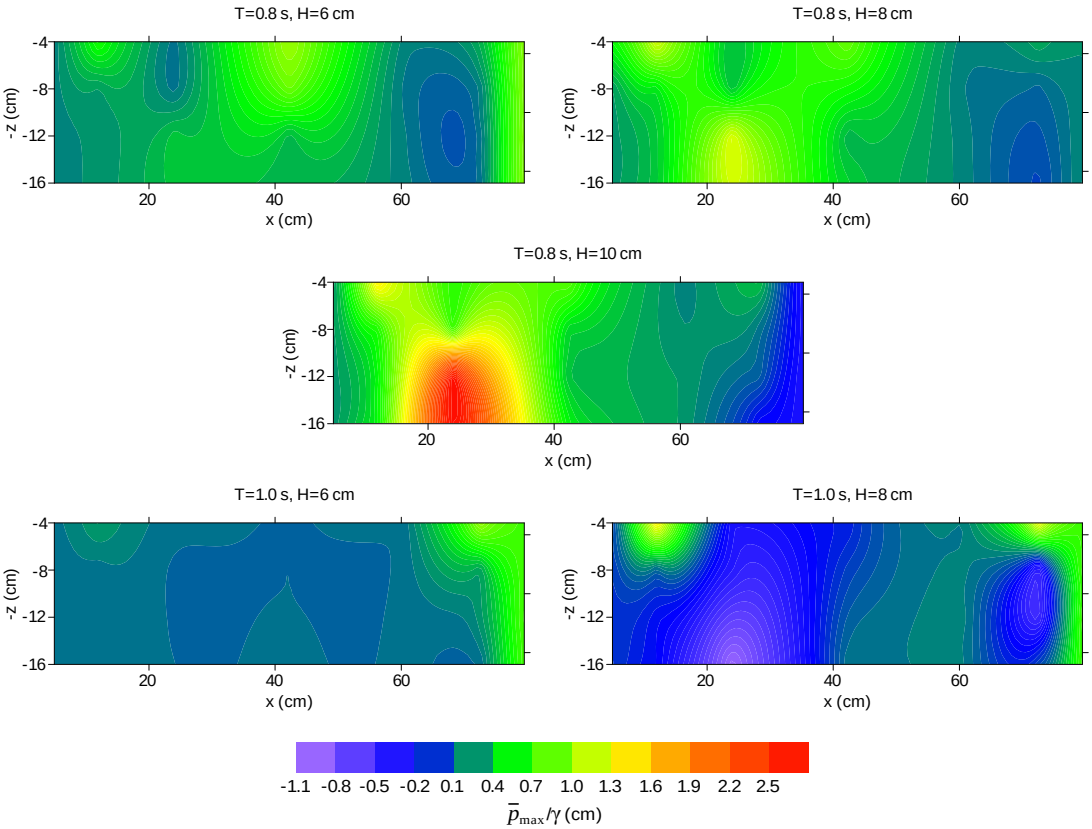

Figure 11. Maximum period averaged pore pressure for Experiment 3 - Phase 1, 85C15A

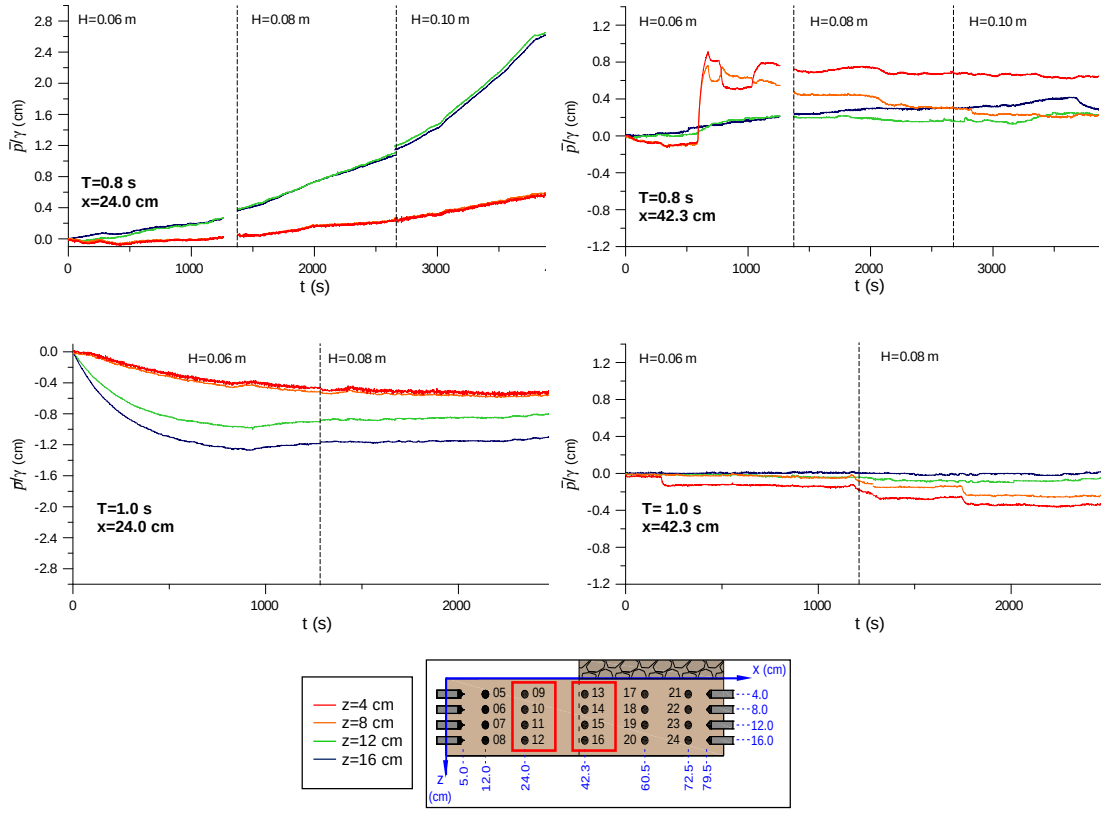

Figure 12. Period averaged pore pressure time-series for Experiment 3 - Phase 1, 85C15A

The time series for this case (Figure 12) show a pore pressure build-up leeward of, and beneath, the structure. In both positions, the pressure reaches a maximum value during the test, and then it is released and tends to stabilize. Leeward of the structure, the pressure loss occurs 60 min after the test started, but below the structure it occurs within the first 20 min of the test.

Another test made with 85C15A was Experiment 4, consisting of four phases, as described in Table 2. The maps in Figure 13 correspond to T = 1.0 s of Phase 4 of the experiment. It can be observed that the highest values beyond the structure were reached at the surface, the opposite to what was observed in Experiment 3. There is a pore pressure build-up beyond the structure, in x = 12 cm (Figure 14). The pressure is released abruptly after 30 min, which may indicate that the mud structure had been broken, but no soil failure (structure sinking) was observed. Also, theoretically, the pore pressure reached during the test is not high enough to cause the failure. In Figure 14, for x = 42.3 cm, at z = 12 and 16 cm, the pore pressure averaged in a wave period tends to decrease in 0.1 cm; on the other hand, long period oscillations (400 s) with low amplitude (0.05 cm) beneath the structure at z = 4 and 8 cm are observed at the same x position. These oscillations show an increasing mean level, indicating periodic pressure accumulation and decrease, nevertheless the overall trend is of increase. This behaviour was observed in other tests with the same soil; results which are completely different from those observed for the other muds. For x=79.5, no pore pressure variation was observed.

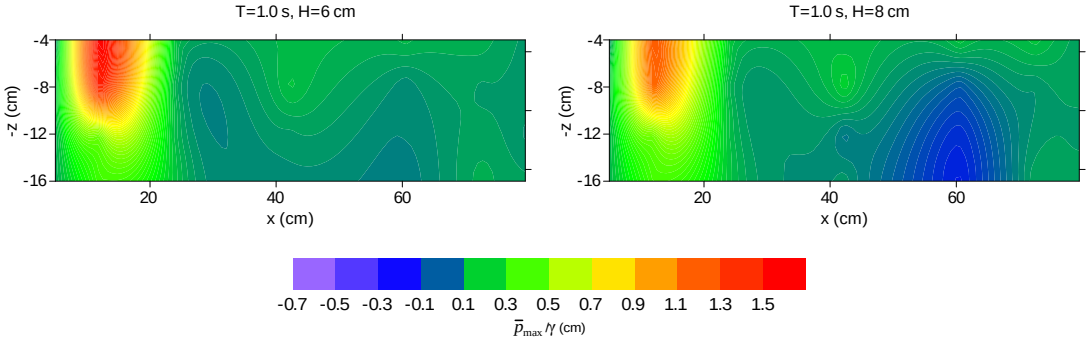

Figure 13. Maximum period averaged pore pressure for Experiment 4 - Phase 4, 85C15A

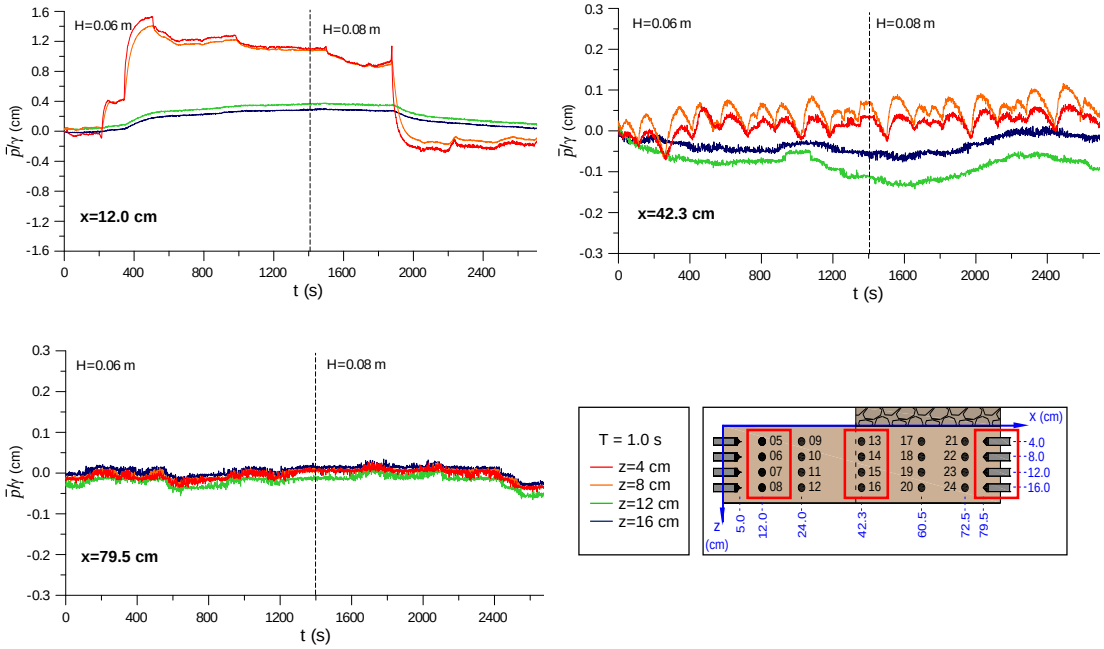

Figure 14. Period averaged pore pressure time-series for Experiment 7 - Phase 1, 90C10A

CONCLUSIONS

In the tests carried out, the build-up present in 85 % mud indicates the possibility of failure, although the pore pressure was released before the critical value that would induce soil liquefaction was reached.

More energetic conditions (higher waves) may prevent the release of the pore pressure, but, because of the experimental facility dimensions, it was not possible to generate higher waves. On the other hand, it is foreseen that if the structure is allowed to rotate around the *Y* axis (perpendicular to the wave propagation direction), as a result of the wave action, the shear stresses generated in the soil will increase. If that happens, mud failure may occur due to the dynamic overloads induced by waves and the structure.

For higher mud contents soil permeability decreases, and thus the possibility for pore water to move through the soil. In this sense, an increase of pore pressure was expected for 90 % and 100 % mud contents, but only pore pressure falls were registered. In soils with higher granular material content, consolidation stabilizes faster and pore pressure accumulation is possible, but in this case the consolidation process, enhanced by the dead weight, favoured pore water drainage. Furthermore, a homogeneous distribution of the pore pressure along the vertical axis and no build-up were observed under the experimental conditions, thus failure only occurred for the soil of 85 % mud content. This absence of pore pressure build-up may also be attributed to the cohesion effects present in muddy soils, as mentioned in de Groot (2006).

The mud response to the combined action of waves and dead weight (vertical breakwater) remains uncertain. In an experimental study, finding a mud content and a water-solids combination capable of bearing that weight, but at the same time loose enough to be overwhelmed by wave action, is still a milestone. However, the soil-waves-structure interaction must be further investigated and understood, for reliable solutions in coastal design and construction to be proposed.

ACKNOWLEDGMENTS

The authors would like to acknowledge funding from the Consejo Nacional de Ciencia y Tecnología (CONCAYT) through the AREDIS project.

REFERENCES

Chávez, V., Mendoza, E., Silva, R., Meneses, A., Perez, D., Clavero, M., Benedicto, I., and Losada, M.A. 2014. Wave-induced pore pressure states on seabeds with a high mud content, *Book of Proceedings of 3rd IAHR Europe Congress*, 10 pp.

de Groot, M.B., Bolton, M.D., Foray, P., Meijers, P., Palmer, A.C., Sandven, R., Sawicki, A., and Teh, T.C. 2006. Physics of Liquefaction Phenomena around Marine Structures. *Journal of Waterway, Port, Coastal and Ocean Engineering*, ASCE, 132 (4), 227–243.

Jeng, D.S. 2013. *Porous Models for Wave-seabed Interactions*. Springer, Shanghai, 289 pp.

Kirca, V. S. O. (2013): Sinking of irregular shape blocks into marine seabed under wave-induced liquefaction. Coastal Engineering, ELSEVIER, 75, 40-51.

Kudella, M., Oumeraci, H., de Groot, M.B., and Miejers, P. 2006. Large-Scale Experiments on Pore Pressure Generation underneath a Caisson Breakwater, *Journal of waterway, port, coastal, and ocean engineering*, ASCE, 132, 310-324.

Mostafa, A.M., Mizuntani, N., and Iwata, K. 1999. Nonlinear Wave, Composite Breakwater, and Seeabed Dynamic Interaction, *Journal of waterway, port, coastal, and ocean engineering*, ASCE, 125, 88-97.

Puzrin, A.M., Alonso E.E., and Pinyol, N.M. 2010. *Geomechanics of Failures*, Springer, 245 pp.

Petróleos Mexicanos. 2008. *Informes plataforma Usumacinta*. Retrieved in 2013 from http://www.pemex.com/index.cfm?action=content&sectionid=119

Sumer, B.M., Fredsøe, J., Christensen, S., and Lind, M.T. 1999. Sinking/floatation of pipelines and other objects in liquefied soil under waves. *Coastal Engineering*, ELSEVIER, 38, 53-90.

Sumer, B.M., Hatipoglu, F., Fredsøe, J., and Ottesen Hansen, N.E. 2006. Critical flotation density of pipelines in soils liquefied by waves and density of liquefied soils. *Journal of Waterway, Port, Coastal and Ocean Engineering*, ASCE, 132 (4), 252–265.

Zhu, J. 2013. Cnoidal Water Wave Induced Pore Pressure Accumulation in the Seabed, *Advances in Petroleum Exploration and Development*, CSCanada, 6 (1), 58-64.